Prediction of subgap states in Zn and Sn-based oxides using various exchange-correlation functionals

Wolfgang Körner,[1,*] Daniel F. Urban,[1,†] David Muñoz Ramo,[2] Paul D. Bristowe,[2] and Christian Elsässer[1,3]

[1] *Fraunhofer Institute for Mechanics of Materials IWM, Wöhlerstr. 11, 79108 Freiburg, Germany*
[2] *Department of Materials Science and Metallurgy, University of Cambridge, Cambridge CB3 0FS, United Kingdom*
[3] *Institute for Applied Materials, Karlsruhe Institute of Technology, Kaiserstr. 12, 76131 Karlsruhe, Germany*

(Dated: November 6, 2014)

We present a density–functional–theory analysis of crystalline and amorphous Zn- and Sn-based oxide systems which focuses on the electronic defect-states within the band gap. A comparison of these electronic levels reveals that the hybrid functionals PBE0, HSE06 or B3LYP agree with a self-interaction corrected (SIC) local-density approximation functional on *occupied* defect levels when similar treatments of the self-interaction are considered. However, for *unoccupied* levels the hybrid functionals and the SIC approach lead to very different predictions. We show that a prerequisite for the determination of the energetic position of subgap states in these oxides is that a functional needs to predict correctly the electronic band structure over a wide energy range and not just close to the band gap. We conclude that for accurate defect levels an adequate treatment of the self interaction problem is required especially in the presence of nearby metal-metal interactions.

PACS numbers: 71.23.-k,71.55.Jv,71.20.Mq

I. INTRODUCTION

Single-particle subgap states within the electronic band gap determine the physics of semiconducting oxides in many respects. In crystalline ZnO, for example, subgap states cause a characteristic green luminescence.[1] In amorphous oxide semiconductors like a-In-Ga-Zn-O or a-Zn-Sn-O which are used for thin-film-transistor liquid-crystal displays on flexible substrates, these subgap states may be the reason why p-type inversion operations in thin-film-transistors have not been achieved so far.[2] The microstructural origin of the subgap states in a-In-Ga-Zn-O and in other amorphous oxides is currently under debate.[2–10] Theoretical models that determine the energetic positions of electronic levels of defect structures with sufficient accuracy would allow for a better interpretation of experimental results. Moreover, understanding how certain subgap states relate to specific defects may enable ways of modifying these defect levels in a controlled manner.

A commonly used theoretical approach to tackle this challenge is density functional theory (DFT). However, the commonly used local-density approximation (LDA) and generalized-gradient approximation (GGA) of DFT have limited predictive power for the electronic level structure of wide band gap semiconductors because of their inherent artificial self-interaction.[11–17] This motivates the ongoing developments of improved functionals. One approach, for example, aims at removing the artificial LDA self-interaction by a self-interaction correction (SIC)[14,18] within the construction of norm-conserving pseudopotentials. Another way of improving the description of the electronic level structure is to substitute a certain amount of GGA by Hartree–Fock (HF) exchange. Functionals that implement this approach are called hybrid functionals.

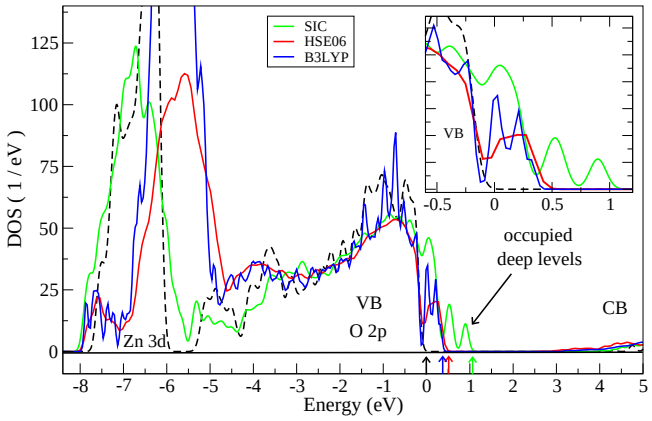

FIG. 1: (Color online) Total DOS of a-Zn_2SnO_4 as calculated with SIC-LDA, HSE06 and B3LYP. The DOS of c-Zn_2SnO_4 with inverse-Spinel ($P4_122$) structure calculated with SIC-LDA is shown for comparison (black dashed line). For HSE06 and B3LYP the Zn 3d bands strongly overlap with the O 2p bands whereas SIC-LDA reproduces well the band separation experimentally observed for ZnO.[14,24] The subgap states extend up to 1 eV for SIC-LDA and to 0.5 eV for HSE06 and B3LYP (see inset). The small arrows on the energy axis indicate the highest occupied levels of the DOS.

Following their introduction substantial testing of hybrid functionals was done concerning lattice constants, bulk moduli, atomization energies, heat of formation and other thermodynamic quantities.[17,19–22] A recent review on ZnO[23] shows that both, hybrid functionals and SIC-LDA lead to considerably improved values for the band gap. However, theoretical predictions of the density of states (DOS) for Zn- and Sn-based oxides obtained using different DFT functionals can vary significantly. This does not only affect the value of the band gap but also

the relative positions of electronic bands and defect levels, which are the focus of this work. To our knowledge, no systematic analysis concerning the defect levels is available so far. The problem is demonstrated in Fig. 1 where the total DOS for an amorphous Zn_2SnO_4 (a-ZTO) structure is shown. The relative positions of the Zn 3d-band with respect to the O 2p band vary substantially. Moreover, there are pronounced differences in the deep levels lying within the band gap of the crystalline reference structure, as shown in the inset of Fig. 1. Details of the calculation are given in the subsequent sections and the results shown in Fig. 1 are discussed in detail in Sec. III. For other amorphous systems such as a-$In_2Zn_2O_5$ (a-IZO, cf. Fig. 2), the agreement between the functionals is found to be much better, as far as the subgap level structure is concerned.

In this work we address the origin of the observed differences by a systematic study of crystalline and amorphous structures, both stoichiometric and with native point defects. As model structures we consider the single crystals of ZnO in the wurtzite structure and SnO_2 in the rutile structure, anion and cation point defects in ZnO and SnO_2, and amorphous structures of In-Zn-O and Zn-Sn-O. We consider the hybrid functionals HSE06, PBE0 and B3LYP[13] and compare the obtained DOS to the results of a SIC-LDA approach.[14]

II. THEORETICAL BACKGROUND

A. Self-interaction

In the Kohn-Sham (KS) formalism of DFT, the one-particle Schrödinger equation in LDA or GGA contains an artificial self interaction.[25] For free atoms the equation reads (in atomic Rydberg units)

$$\left(-\nabla^2 - \frac{2Z}{r} + V_{\rm H}[n] + V_{\rm xc}[n]\right)\Psi_i = \epsilon_i \Psi_i, \qquad (1)$$

where the Ψ_i is the wavefunction and ϵ_i is the energy eigenvalue of the one-electron orbital. The total electron density $n = \sum_i n_i$ is the sum of the partial orbital densities $n_i = p_i|\Psi_i|^2$ where p_i are the orbital occupation numbers. The electrostatic Hartree potential $V_{\rm H}$ and the LDA or GGA exchange-correlation (xc) potential $V_{\rm xc}$ are both evaluated with the total density n, thus the density of each orbital interacts with itself. Unlike in Hartree-Fock theory, however, these Hartree and xc self-interactions do not exactly cancel each other.

One possible procedure to reduce this inherent self-interaction is the construction of pseudopotentials for the valence electrons that contain a self-interaction-correction (SIC) term for each angular-momentum l which is subtracted from the Hartree and xc potentials

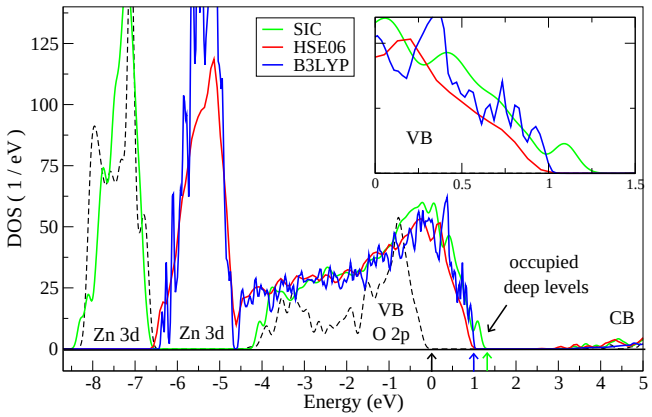

FIG. 2: (Color online) Total DOS of a-$In_2Zn_2O_5$ calculated using SIC-LDA, HSE06 and B3LYP. As reference, the DOS of c-ZnO calculated using SIC-LDA is shown (black dashed line). The three functionals predict almost the same depth of the subgap states but differ in the position of the Zn 3d bands. The small colored arrows on the energy axis mark the highest occupied levels of the DOS.

of the orbital densities as follows:

$$\Big(-\nabla^2 + V_l + V_{\rm H}[n_v] + V_{\rm xc}[n_v] - \underbrace{\Big[V_{\rm H}[n_l] + V_{\rm xc}[n_l]\Big]}_{:=V_{\rm cor}[n_l]}\Big)\Psi_l^{pp} = \epsilon_l^{pp}\Psi_l^{pp} \qquad (2)$$

where n_v is the pseudodensity of all valence electrons $n_v = \sum_l n_l$ and $n_l = p_l|\Psi_l^{pp}|^2$ is the pseudodensity of orbital l and $V_l(r)$ are norm-conserving ionic pseudopotentials for the valence electrons (for instance by the scheme proposed by Vanderbilt.[26]). Further details of this approach and its extension to solids can be found in Refs. 14 and 18.

B. Hybrid-Functionals

Another approach that reduces the self interaction problem of LDA or GGA is the partial incorporation of Hartree-Fock (HF) exchange which itself by construction is self-interaction free. The PBE0 functional, for example, mixes 75% of semilocal GGA-PBE exchange and 25% of nonlocal HF exchange where the partition has been justified by means of Görling-Levy perturbation theory.[27] A conceptually similar hybrid functional is B3LYP which in contrast includes heuristic fitting parameters.[28] The computation of the non-local HF exchange is computationally very demanding due to its long-range character. This has led to the development of the semi-empirical functional HSE06 containing a separation of the exchange energy into a short-range and a long-range part which are computed with PBE0 and GGA, respectively.[29,30] A concise overview of the three hybrid functionals can be found in Ref. 13.

The admixture of HF exchange to a given DFT xc-functional is conceptually rather different from the SIC described in the previous subsection. While the SIC is only applied to occupied orbitals[14,18,31] the HF exchange potential acts on all orbitals irrespective of their occupation. Depending on the system under investigation this can give rise to substantial differences in the energy levels of the subgap states. In this work we will show that when the states are occupied they only shift in energy but when they are unoccupied they can be qualitatively different, i.e. present or absent.

III. RESULTS AND DISCUSSION

The inconsistent results concerning the deep defect levels found for the amorphous oxide semiconductors shown in the introduction suggest the following systematic analysis. We have selected a set of amorphous and crystalline structures which vary in atomic composition and stochiometry. These give rise to band structures with varying degrees of band overlap, and to different types of defect states of varying localization which are either occupied or unoccupied. For the atomistic structures considered we have determined the electronic DOS with the SIC-LDA, HSE06, PBE0 and B3LYP functionals. Computational details are summarized in the appendix. We used identical atomistic structures as input data for the different functionals, namely those optimized using LDA. One exception is the a-IZO structure which was optimized with B3LYP.

In general, the hybrid functionals systematically produce larger lattice parameters than LDA.[11,32] This has the effect that DOS calculations for LDA–optimized structures yield slightly larger band widths than for the structures determined with hybrid functionals. This effect is of order 0.1 eV and thus negligible for our analysis of subgap states. However, the band gaps can vary by up to 0.5 eV when taking optimized parameters from LDA rather than from hybrid functionals. We are aware of this point but have found that the (deep) occupied states do not depend on the band gap. B3LYP and PBE0 which produce larger band gaps than HSE06 for all oxides considered in this work[33] lead to very similar or even identical *occupied* levels. Note that the conduction band edge is determined by *unoccupied* levels which, as will be shown later, have to be interpreted with caution when calculated with the hybrid functionals.

Furthermore, for some point-defect structures we examined explicitly how much atomic relaxation (e.g. using HSE06) modifies the electronic structure compared with the LDA-relaxed result. We found that the DOS is not qualitatively changed by relaxation and the comparison between the functionals remains the same. For example, occupied defect levels calculated with SIC-LDA are higher in energy than the defect levels obtained by the hybrid functionals. In general, the effect of atomic relaxation on the electronic levels of the DOS using an individual functional is 0.3 eV at most.

Note that for our model structures the defect levels of B3LYP are always found to be 0.1 eV lower than those obtained by HSE06 and PBE0 whereas for all occupied states we have analyzed, the PBE0 and HSE06 approaches yield exactly the same result. By contrast, the energies of unoccupied states are at least 0.5 eV lower for HSE06 compared to PBE0, and hence similar to the differences in the corresponding band gaps.

For each given bulk crystal structure we have aligned the DOS obtained with the different functionals according to the valence band (VB) edge which is set to 0 eV in all our figures. For the comparison of the positions of the subgap states of the point-defect and amorphous structures we have aligned the DOS of the structures containing defects with the DOS of the perfect single crystals using levels that lie far below the band gap region.

A. Zn 3d-band

The comparison of the total DOS of a-Zn_2SnO_4 calculated with SIC-LDA, HSE06, and B3LYP, as shown in Fig. 1, reveals that the functionals not only differ in their prediction of subgap states but also disagree on the position of the Zn 3d-band. The hybrid functionals show a strong overlap of the Zn 3d band with the O 2p band while SIC-LDA produces a band separation similar to that observed and calculated in ZnO.[14,24] Although no experimental data are available for a-Zn_2SnO_4, it is reasonable to conjecture that the Zn 3d and O 2p bands are separate in this oxide as well since the full Sn 4d band will be very low lying. The occupied Zn 3d states which are strongly localised are a good benchmark of how well the self-interaction is corrected by a functional and Fig. 1 suggests that the hybrid functionals do not fully correct the error of the self-interaction.

A second material displaying the difficulty of the Zn 3d band position is a-$In_2Zn_2O_5$ for which the DOS is shown in Fig. 2. For the SIC-LDA the 3d and 2p bands are well separated. The hybrid functionals again place the Zn 3d band apparently too close to the O 2p band but in this case, there is not such a substantial band overlap as seen for a-Zn_2SnO_4 (see Fig. 1).

B. Metal vacancies in crystalline and amorphous phases

Both stoichiometric amorphous structures considered so far, a-Zn-Sn-O in Fig. 1 and a-In-Zn-O in Fig. 2, contain a defect which can be described as either a metal vacancy or an undercoordinated oxygen atom.[8,9] Defects of this kind lead to occupied defect levels which are superimposed on the broad valence band (VB) tail. In Fig. 2 it can be seen that the different functionals yield almost the same distribution of deep occupied levels above the VB except for a slightly deeper level predicted by the

SIC approach. An analysis of the local DOS of the individual atoms shows that about half the contribution to these levels comes from a single undercoordinated oxygen atom.

For the amorphous Zn-Sn-O model the hybrid functionals predict deep levels that extend to about 0.5 eV above the VB whereas the SIC approach yields deep levels which are found up to about 1 eV. About 73% of the contribution to the deepest levels comes from a single undercoordinated oxygen atom in the supercell. All functionals relate the deep levels to the same undercoordinated oxygen atom but their energies relative to the VB edge differ by a factor of two, corresponding to 0.5 eV.

Why do we obtain almost quantitative agreement between the different functionals for a-In-Zn-O whereas for a-Zn-Sn-O it is only qualitative? The position of the Zn 3d band in a-In-Zn-O differs strongly for the different functionals. Based on the results for ZnO discussed in the previous subsection, SIC appears to place the Zn 3d levels at about the right depth relative to the VB edge while the other three functionals produce Zn 3d-bands which are significantly too high in energy. Nevertheless, there is only a slight overlap with the O 2p levels which form the VB (see Fig. 2). The situation is similar for a-Zn-Sn-O but here the three hybrid functionals yield a strong overlap between the Zn 3d band and the O 2p band. This implies a strong artificial 3d-2p interaction. The SIC approach on the other hand leads to well separated Zn 3d and O 2p bands.

For comparison, we examine a model system which is Zn-free and therefore does not have the difficulty of the band separation discussed above. We consider metal vacancies in crystalline SnO_2 which result in locally undercoordinated oxygen atoms. Depending on the electron chemical potential this point defect prefers different charge states. We found a very large variation in subgap states depending on the charge state of the defect. We begin with a charged defect state which shows occupied defect levels in contrast to the uncharged state which shows essentially unoccupied defect levels. This will be discussed subsequently.

In Fig. 3 (a) the defect levels of the tin vacancy (V_{Sn}) in SnO_2 in the charged state ($q = -2$) are shown. The hybrid functionals predict occupied levels close to the VB edge and unoccupied deep levels within the band gap. The SIC approach agrees with the position of the occupied levels but does not show unoccupied deep levels within the band gap. The good agreement concerning the occupied defect levels is consistent with the results for the amorphous structures discussed above. Without the overlap problem of the Zn 3d band and O 2p band the energies of the occupied gap levels determined with the four functionals agree quantitatively.

The disagreement concerning the unoccupied levels gets worse when the tin vacancy in SnO_2 is in the neutral charge state (q=0), see Fig. 3 (b). The three hybrid functionals yield unoccupied deep levels distributed over

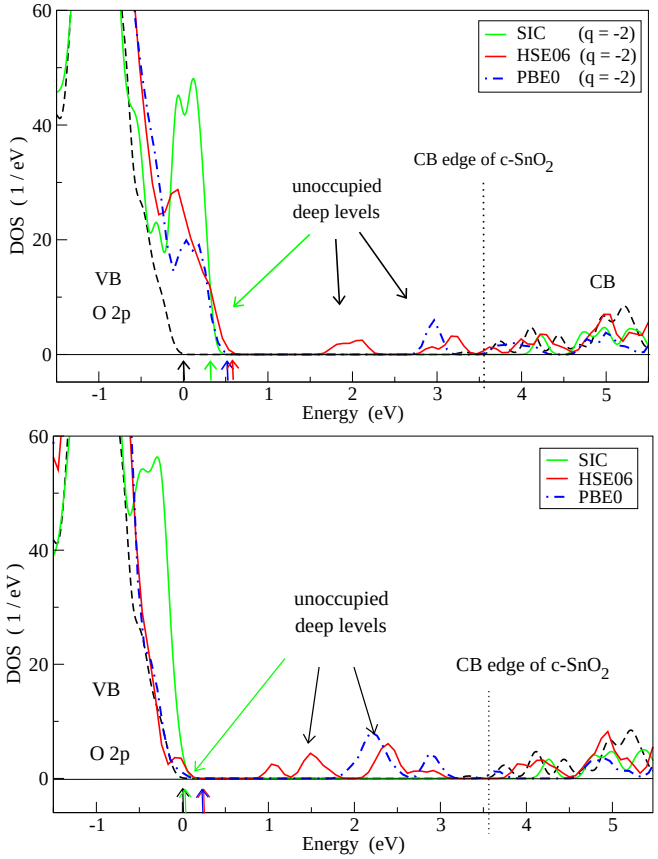

FIG. 3: (Color online) Total DOS of c-SnO_2 containing a tin vacancy (V_{Sn}) in (a) charge state $q = -2$ and (b) neutral state $q = 0$. The DOS of bulk SnO_2 obtained with SIC-LDA is shown for comparison (black dashed line) The different functionals agree quantitatively on the position of the occupied subgap states. However, the hybrid functionals predict unoccupied states distributed over most of the band gap whereas the SIC approach predicts unoccupied states only at the VB tail (see long green arrow).The small colored arrows on the energy axis mark the highest occupied levels of the DOS.

the whole gap whereas the SIC-LDA approach predicts unoccupied levels close to the VB edge (indicated by the long green arrow in Fig. 3b). The results of the hybrid functionals and SIC obviously disagree qualitatively. The results of the two hybrid functionals vary strongly (by about 0.5 eV) such that the unoccupied defect levels are shifted to higher energies for larger predicted band gaps (E_{gap}(PBE0) = 3.43 eV; E_{gap}(HSE06) = 2.66 eV).

For a zinc vacancy in ZnO the situation is very similar. In the charge neutral state we obtain a result like Fig. 3 in which the hybrid functionals predict unoccupied defect levels spread over the band gap. Adding electrons leads to occupied defect levels just above the VB edge. The SIC approach predicts unoccupied levels directly above the VB for the charge neutral defect which are filled and extend up to 1.3 eV for charge state q = -2. The only difference compared to Fig. 3 (a) is that the occupied defect levels from SIC reach deeper into the band gap than

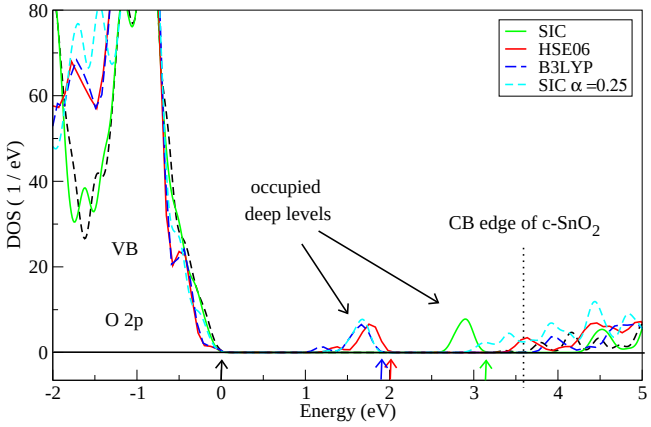

FIG. 4: (Color online) Total DOS of c-SnO_2 containing an oxygen vacancy (V_O) in the charge neutral state. HSE06, B3LYP and the reduced SIC with $\alpha = 0.25$ (see text) almost agree on the position of the occupied defect level while SIC-LDA puts it about 1 eV higher. The DOS of bulk SnO_2 obtained by SIC-LDA is shown for comparison (black dashed line). The small arrows on the energy axis mark the highest occupied levels of the DOS.

the occupied levels from the hybrid functionals (only up to 0.5 eV for charge state q = -2) . This again is consistent with the finding that subgap states obtained by the hybrid functionals are significantly lower in energy than for the SIC if the corresponding Zn 3d bands strongly overlap with the O 2p bands.

C. Oxygen vacancies in crystalline and amorphous phases

After having examined the defect states caused by a metal vacancy or an undercoordinated oxygen atom we now turn to oxygen vacancies. For the amorphous structures, a configuration corresponding to an oxygen vacancy in a crystal structure is a local oxygen deficiency[8,9] resulting, e.g., in a metal-metal defect structure such as a Sn-Zn defect in a-Zn-Sn-O. The Sn-Zn defects are characterized by a Sn and a Zn atom in close vicinity which are not separated by an oxygen atom.

Fig. 4 shows the defect levels of the oxygen vacancy in c-SnO_2. There is a substantial disagreement on the position of the occupied deep levels as predicted by the different functionals, although the problem of overlapping Zn 3d and O 2p bands is naturally absent. The hybrid functionals lead to defect levels at about 1.75 eV above the VB-edge compared to 2.8 eV for SIC-LDA. From this we conclude, that when considering metal-metal defect structures, the ill-positioned Zn 3d bands are not the only reason for the different results. The large difference in energy levels of about 1 eV is most probably connected to the way a local metal-like atomic arrangement is treated by the functionals.

This conjecture is supported by further insight supplied by the study of the oxygen vacancy in ZnO. Here, the SIC approach yields defect levels at 2.2 eV[14] above the VB edge. The three hybrid functionals on the other hand place the deep levels due to the oxygen vacancy at about 0.6 eV. The large difference of about 1.6 eV between the positions of the deep levels obtained with the hybrid functionals and with the SIC approach can be thought of as the superposition of two effects, one due to the Zn 3d - O 2p band overlap giving a difference of about 0.5 eV in defect level position and the other due to metal-metal proximity adding a further 1 eV.

Finally we consider amorphous $ZnSnO_3$. Fig. 5 shows the subgap states for a Sn-Zn defect in a-$ZnSnO_3$+V_O where V_O denotes an oxygen vacancy. The hybrid functionals predict occupied deep levels which are at about 1 eV above the VB edge whereas the SIC-LDA approach places them at about 2.5 eV. The situation is very similar to that found for the oxygen vacancy in c-ZnO. Again we relate the difference of about 1.5 eV between the energy levels obtained with the hybrid functionals and with the SIC approach to the combined effects of band overlap and metal-metal interaction.

The impact of the admixture of HF exchange can be seen by varying the mixing parameter a determining the fraction of HF exchange in the HSE06 functional. For the oxygen vacancy in ZnO an increase of a from 0.25 to 0.375 moves the defect levels up in energy to almost 1 eV above the VB edge accompanied by a down-shift of the Zn 3d band position by about 0.6 eV. This is also reported in Ref. 32 in which the value of a=0.375 was obtained by adjusting the HSE band gap to the experimental value. The larger band gap using HSE with a=0.375 does not seem to be the key for obtaining higher V_O defect levels since PBE0, which yields almost the experimental band gap value, places the occupied V_O defect levels exactly as HSE06 does with a=0.25. Apparently, the crucial point is that the calculation with a=0.375 reduces the artificial overlap of the Zn 3d and O 2p bands.

Interestingly, the positions of the defect levels obtained by the hybrid functionals can be reproduced with an artificially *reduced* SIC. Setting the SIC-parameter α to 0.25 corresponds to a SIC of only 25% relative to isolated atoms (see Sec. VI). For all *occupied* defects for which we considered this setting, SIC yields defect levels at the same positions as the hybrid functionals and thus mimics the incorporation of 25% HF exchange in the hybrid functionals (cf. Figs. 4 and 5).

D. Discussion

Perdew and Zunger showed that a self-interaction free theory leads to electronic band structures that are close to the real single particle levels and stated that: *HF is a self-interaction free theory for the occupied states but due to the lack of correlation and the inclusion of spurious self interaction for the unoccupied states fails to predict correct band gaps.*[25] The admixture of HF ex-

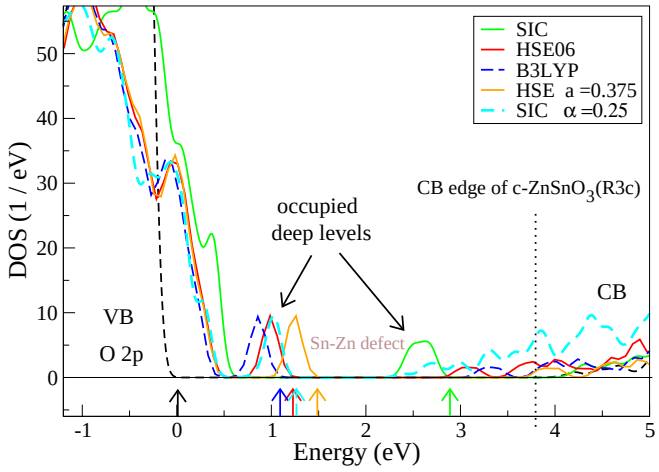

FIG. 5: (Color online) Total DOS of a-$ZnSnO_3$:V_O as calculated with SIC, HSE06, B3LYP, HSE with $a = 0.375$ and SIC with $\alpha = 0.25$. The DOS of c-$ZnSnO_3$ (R3c structure) calculated using SIC-LDA is shown for comparison (black dashed line). The hybrid functionals HSE06 and B3LYP predict subgap states in the lower half of the band gap. SIC puts the energetic position of this occupied oxygen-vacancy-like defect significantly higher while the reduced SIC with $\alpha = 0.25$ agrees with the hybrid functionals. Increasing the HF contribution moves all occupied and unoccupied levels higher in energy. The small arrows on the energy axis mark the highest occupied levels of the DOS.

change into DFT functionals increases the splitting of the occupied and unoccupied states which often results in more satisfactory values for band gaps. However, the self-interaction correction provided by 25% HF exchange is apparently not sufficient. Highly localized bands like Zn 3d are a prominent example. What is the effect of the spurious band overlap predicted by the hybrid functionals? We tested this by continuously reducing the amount of SIC used in the SIC-LDA scheme. An artificial reduction of the self-interaction correction to just 25% (by setting the SIC parameter $\alpha = 0.25$) shows that the 3d levels move up in energy and approach the O 2p band. Finally, when the overlap is large enough the 3d band pushes up the O 2p band which also has the effect of reducing the band gap. We have employed the same artificially reduced SIC for all the defect structures considered in this work and the subgap levels are always found to agree quantitatively with the results of the hybrid functionals. We therefore conclude, that the inadequate correction of self-interaction via the incorporation of 25% HF exchange is a major cause of the effects discussed in this paper.

Thus we conjecture that for the hybrid functionals the too high lying Zn 3d band pushes up the O 2p levels which perturb and superimpose the energies of the defect levels connected to the undercoordinated oxygen atoms. This mechanism may explain why the subgap states of the hybrid functionals lie too low relative to the VB edge.

For the unoccupied defect levels we have found a quantitative and qualitative difference between the hybrid functionals and SIC. While for the perfect crystalline structures the hybrid functionals and the SIC approach come to similar CB edges and thus similar band gaps, the situation is most inconsistent for the Sn and Zn vacancies. On the one hand the SIC approach predicts unoccupied states directly at the VB edges and thus a metallic situation (see Figs. 3 (a) and (b)). On the other hand the hybrid functionals predict large energy differences between occupied and unoccupied states. Hence, unoccupied deep levels in oxide semiconductors predicted by the hybrid functionals should be interpreted with caution.

system	defect	Zn(3d)-O(2p) splitting	metal-metal configuration	ΔE_{occ} (in eV)
a-$ZnSnO_3$	V_O	yes	yes	1.6
c-ZnO	V_O	yes	yes	1.6
c-SnO_2	V_O	no	yes	1.05
a-Zn_2SnO_4	O_{uc}	yes	no	0.5
a-$In_2Zn_2O_5$	O_{uc}	yes	no	0.25
c-ZnO	V_{Zn}^{-2}	yes	no	0.7
c-SnO_2	V_{Sn}^{-2}	no	no	0.0

TABLE I: Summary of the considered systems containing undercoordinated oxygen atoms (O_{uc}), oxygen vacancies (V_O) or charged metal vacancies (V_{Zn}^{-2}, V_{Sn}^{-2}). In the case of a-$ZnSnO_3$ V_O denotes a local oxygen deficiency. ΔE_{occ} is the energy difference between the occupied defect levels obtained by SIC-LDA and the hybrid functionals.

IV. SUMMARY

We have studied the electronic densities of states of crystalline and amorphous Zn- and Sn-based oxides using the hybrid functionals HSE06, B3LYP and PBE0 and a SIC-LDA approach. The three hybrid functionals, compared among each other, lead to similar results for *occupied* subgap states and show differences mainly in the energies of *unoccupied* states. Comparing the hybrid results with those of SIC shows that the latter differ in many cases only by a shift in energy when the *occupied* subgap states are considered. If the treatment of the self-interaction is modified by adjusting the scaling/mixing parameters in the different approaches then the agreement improves. However, for the *unoccupied* subgap states the disagreement between the functionals is more substantial and can result in the presence or absence of states from the band gap.

Table I summarizes our results concerning the occupied subgap states. We relate the energy difference ΔE_{occ} between the defect levels obtained by SIC-LDA

and the hybrid functionals to two main factors, (1) the artificial interaction between Zn 3d and O 2p bands when they are not separated enough in energy, and (2) local metal-metal configurations.

Factor (1) is relevant for all our structures containing Zn and causes an upshift in energy of the subgap-level positions of about 0.5 eV for the hybrid functionals, compared to the results of the LDA-SIC approach for which the Zn 3d and O 2p bands are always well separated.

Factor (2) is relevant when considering oxygen vacancies in crystalline structures or local oxygen deficiencies in amorphous systems, which result in metal-metal defect structures. For these systems we observe an additional separation in subgap-level position of approximately 1eV when comparing the hybrid functionals to SIC-LDA.

Furthermore, we have found that for uncharged metal vacancies in ZnO and SnO_2, the hybrid functionals show unoccupied defect levels widely spread over all the band gap which change qualitatively and quantitatively when filled by additional electrons (charged defect states). This effect, which seems physically unreasonable, is not exhibited by SIC-LDA suggesting that the latter approach is more reliable in this case. Ultimately, however, deciding which approach is superior relies on the availability of good quality spectroscopic data on the specific defects and oxides under consideration.

In conclusion, current approaches beyond LDA and GGA, namely hybrid functionals and SIC-LDA pseudopotentials considered in this work, unfortunately do not agree on subgap states in Zn- and Sn-based oxides and the reliable prediction of electronic defect levels remains a difficult task. Essential to the calculation of precise defect levels is a sufficiently accurate treatment of the self-interaction problem especially in the presence of nearby metal-metal interactions.

V. ACKNOWLEDGMENTS

Financial support for this work was provided by the European Commission through contract No. NMP3-LA-2010-246334 (ORAMA). The calculations at Cambridge were performed using the High Performance Computing Facility, Darwin, and also the UK national high performance computing service ARCHER, for which access was obtained via the UKCP consortium and funded by EPSRC grant EP/K014560/1.

VI. APPENDIX: COMPUTATIONAL DETAILS

A. SIC-LDA calculations

The electronic-structure calculations on the basis of SIC-LDA were performed using the computational mixed basis pseudopotential (MBPP) method[34–37] with the same calculation setup as in previous papers.[8–10,14,15] We have taken the LDA for exchange-correlation as parameterized by Perdew and Zunger.[25] For Sn, In, Ga, Zn, and O optimally smooth norm–conserving pseudopotentials[26] were constructed, and a mixed–basis of plane waves and non-overlapping localized orbitals are used. Due to the localized orbitals a plane–wave cutoff energy of 20 Ry (1Ry = 13.606 eV) is sufficient to obtain converged results. For the k-point sampling of the Brillouin-zone integrals Monkhorst-Pack meshes of $3 \times 3 \times 3$ and a Gaussian broadening of 0.2 eV were used. The DOS of the supercells were evaluated with the same meshes and a Gaussian smearing of 0.1 eV.

The self-interaction of LDA is reduced by an implementation of the SIC in the pseudopotentials.[14,18] This does not require more computational effort and thus is applicable to supercells of about 100 atoms.

The SIC procedure uses the weight factors (w_s, w_p, w_d) accounting for occupation of the individual s, p and d valence orbitals. We corrected the In 4d, Sn 4d and Zn 3d orbitals by 100% using In(0, 0, 1), Sn(0, 0, 1), Zn(0, 0, 1). The localized O 2s semi-core orbitals are also corrected by 100% while for the spatially more extended O 2p valence orbitals we have taken O(1, 0.8, 0) for ZnO and O(1, 0.93, 0) for SnO_2 in order to obtain good band gap values.[9] The different values have their origin in the change from fourfold tetrahedral coordination in the wurtzite structure of ZnO to sixfold octahedral coordination in the rutile structure of SnO_2. For the ternary crystalline and amorphous Zn-Sn-O and In-Zn-O compounds we have chosen O(1, 0.9, 0). This intermediate value of 90% correction of the O 2p orbitals is chosen to take into account the presence of both coordinations in these structures. The adequacy of that choice was shown for Zn-Sn-O in Ref. 9.

For the application of the SIC to solids, we have reduced the atomic SIC by a factor $\alpha = 0.8$ for all the oxides considered in this paper which leads to excellent band structures for c-ZnO, c-SnO_2, c-$ZnSnO_3$ and c-Zn_2SnO_4.[8,9,14]

For some calculations we used a *reduced* SIC with $\alpha = 0.25$ in order to mimic the 25% HF exchange of the hybrid functionals.

B. HSE06 and PBE0 calculations

The calculations with HSE06 and PBE0 which are based on the Perdew-Burke-Ernzerhof (PBE) GGA functional[38] were performed using the projector augmented-wave (PAW) method[39] as implemented in the VASP code.[40,41] The Zn 3d, 4s, 4p, O 2s, 2p, Sn 4d, 5s, 5p and In 4d, 5s, 5p were described as valence electrons. A plane-wave cutoff energy of 400 eV and a $2 \times 2 \times 2$ k-mesh were used. For some supercells test calculations with a $4 \times 4 \times 4$ k-mesh and a plane-wave cutoff energy of 500 eV were performed which confirmed a sufficient convergence of the DOS for the lower parameters. The DOS of the supercells were evaluated with the same k-mesh

	structure	a [Å]	c [Å]	u	N
SnO_2	rutile ($P4_2mnm$)	4.81	3.21	0.307	72
ZnO	wurtzite ($P6_3mc$)	3.23	5.16	0.380	72
Zn_2SnO_4	inverse-spinel[42] ($P4_122$)	8.62		0.383	56
$ZnSnO_3$	$LiNbO_3$[43] (R3c)	5.29	14.1	0.286	64

TABLE II: Optimised lattice parameters a and c and internal parameter u for crystalline SnO_2, ZnO, Zn_2SnO_4 and $ZnSnO_3$ obtained using LDA and supercells containing N atoms.

and a Gaussian smearing of 0.1 eV. The mixing parameter a determining the fraction of HF exchange was kept at 0.25. For some calculations we increased it to 0.375 in order to expose the effect of the HF admixture on the gap states.

C. B3LYP calculations

The B3LYP calculations were performed with the CRYSTAL09 code[44], which uses a localized basis set to alleviate the computational requirements of the calculations. Oxygen has a basis set consisting of 14s, 6p, and 1d functions contracted to 1s, 3sp, and 1d. For the cations, we use relativistic effective core potentials (RECP) again to reduce the computational cost. For Zn, we use a RECP of Stevens et al.[45] that replaces all but 10 valence electrons. The related basis set consists of 8 sp and 6 d functions contracted to 3 sp and 2 d shells. A RECP of Stevens et al.[45] is also used for In, with 21 valence electrons and a related basis set of 8 sp and 5 d functions contracted to 4 sp and 3 d shells.

D. Crystalline and amorphous supercell models

As reference and starting point for the generation of the amorphous model systems we constructed the crystalline supercells listed in Tab. II. The crystalline ZnO and SnO_2 structures containing oxygen, zinc or tin vacancies and the amorphous Zn-Sn-O strutures were structurally relaxed using LDA by optimizing the atomic positions according to the Broyden-Fletcher-Goldfarb-Shanno (BFGS) algorithm.[46]

The amorphous structures where generated by means of classical molecular-dynamics (MD) simulations with the GULP code.[47] Empirical rigid-ion potentials of Buckingham type were employed. The MD simulations were started by melting the crystal at 5000 K and subsequently cooling the melt to down in steps of 10 K per ps with time steps of 2 fs at constant temperature and constant volume. Finally, the obtained structures were relaxed using LDA with the BFGS algorithm.

In order to study non-stoichiometric amorphous structures we removed single atoms from the individual amorphous supercells and relaxed subsequently by LDA calculations.

The amorphous IZO supercell with 12 indium, 12 zinc and 30 oxygen atoms was created differently by means of a melt-quench procedure using classical MD over a large cell, followed by selection of a small sub-cell from the large model and further refinement of this structure with a Reverse Monte–Carlo technique.[48] The MD simulations were performed using DLPOLY code.[49]

* Electronic address: wolfgang.koerner@iwm.fraunhofer.de
† Electronic address: daniel.urban@iwm.fraunhofer.de

[1] Y.W. Heo, D.P. Norton, S.J. Pearton, J. Appl. Phys. **98**, 073502 (2005).
[2] K. Nomura, T. Kamiya, H. Yanagi, E. Ikenaga, K. Yang, K. Kobayashi, M. Hirano and H. Hosono, Appl. Phys. Lett. **92**, 202117 (2008).
[3] H.-H Hsieh, T. Kamiya, K. Nomura, H. Hosono and C.-C. Wu, Appl. Phys. Lett. **92**, 133503 (2008).
[4] M. Kimura, T. Nakanishi, T. Kamiya, K. Nomura and H. Hosono, Appl. Phys. Lett. **92**, 133512 (2008).
[5] K. Nomura, T. Kamiya, E. Ikenaga, H. Yanagi, K. Kobayashi and H. Hosono, J. Appl. Phys. **109**, 073726 (2011).
[6] T. Kamiya, K. Nomura, M. Hirano and H. Hosono, Phys. Stat. Sol. C **5**, 3098 (2008).
[7] T. Kamiya, K. Nomura and H. Hosono, Phys. Stat. Sol. A **206**, 860 (2009).
[8] W. Körner, P. Gumbsch and C. Elsässer, Phys. Rev. B **86**, 165210 (2012).
[9] W. Körner and C. Elsässer, Thin Solid Films **555**, 81 (2014).
[10] W. Körner, D. F. Urban and C. Elsässer, J. Appl. Phys., **114**, 163704 (2013).
[11] J. Heyd, J. E. Peralta, G. E. Scuseria and R. L. Martin, J. Chem. Phys. **123**, 174101 (2005).
[12] A. V. Krukau, O. A. Vydrov, A. F. Izmaylov and G. E. Scuseria, J. Chem. Phys. **125**, 224106 (2006).
[13] M. Marsman, J. Paier, A. Stropa and G. Kresse, J. Phys.: Condens. Matter **20**, 064201 (2008).
[14] W. Körner and C. Elsässer, Phys. Rev. B **81**, 085324 (2010).
[15] W. Körner and C. Elsässer, Phys. Rev. B **83**, 205306 (2011).
[16] P. Rinke, A. Janotti, M. Scheffler and C. G. Van de Walle, Phys. Rev. Lett. **102** , 026402 (2009).
[17] S. J. Clark, J. Robertson, S. Lany and A. Zunger, Phys. Rev. B **81**, 115311 (2010)
[18] D. Vogel, P. Krüger and J. Pollmann, Phys. Rev. B **54**, 5495 (1996).
[19] J. Paier, M. Marsman and G. Kresse, J. Chem. Phys. **127**, 024103 (2007).
[20] P. Agoston, K. Albe, R. M. Nieminen and M. J. Puska,

Phys. Rev. Lett. **103**, 245501 (2009).
[21] S. Lany and A. Zunger, Phys. Rev. Lett. **106**, 069601 (2011).
[22] P. Agoston, K. Albe, R. M. Nieminen and M. J. Puska, Phys. Rev. Lett. **106**, 069602 (2011).
[23] F. Oba, M. Choi, A. Togo and I. Tanaka, Technol. Adv. Mater. **12**,034302 (2011).
[24] *Semiconductors Physics of Group 4 Elements and 3-5 Compounds*, edited by K. H. Hellwege and O. Madelung, Landbolt-Börnstein, New Series, Group 3, Vol. 17, Pt. a (Springer, Berlin 1982); *Semiconductors. Intrinsic Properties of Group 4 Elements and 3-5-7, and 1-7 Compounds*, edited by K. H. Hellwege and O. Madelung, Landolt-Börnstein, New Series, Group 3, Vol 22, Pt. a (Springer, Berlin 1987).
[25] J. P. Perdew and A. Zunger, Phys. Rev. B **23**, 5048 (1981).
[26] D. Vanderbilt, Phys. Rev. B **32**, 8412 (1985).
[27] J. P. Perdew, M. Ernzerhof, and K. Burke, J. Chem. Phys. **105**, 9982 (1996).
[28] Gaussian NEWS Vol 5(2), 2, (Gaussian Inc., Pittsburgh, PA 1994).
[29] M. Enzerhof and G. E. Scuseria, J. Chem. Phys. **110**, 5029 (1999).
[30] C. Adamo and V. Barone, J. Chem. Phys. **110**, 6158 (1999).
[31] The statement that the SIC only applies to occupied levels refers to the construction of the pseudopotentials. Nevertheless, the self-interaction corrections according to occupation numbers of the orbitals are chosen such that they are close to the average values of the considered compounds.
[32] F. Oba, A. Togo, I. Tanaka, J. Paier and G. Kresse, Phys. Rev. B **77**, 245202 (2008).
[33] S. L. Lany and A. Zunger, Phys. Rev. Lett. **106**, 069601 (2011).
[34] C. Elsässer, N. Takeuchi, K. M. Ho, C. T. Chan P. Braun and M. Fähnle, J. Phys.: Condens. Matter **2**, 4371 (1990).
[35] K. M. Ho, C. Elsässer, C. T. Chan and M. Fähnle, J. Phys.: Condens. Matter **4**, 5189 (1992).
[36] B. Meyer, K: Hummler, C. Elsässer and M. Fähnle, J. Phys.: Condens. Matter **7**, 9201-9217 (1995)
[37] F. Lechermann, M. Fähnle, B. Meyer and C. Elsässer Phys. Rev. B **69**, 165116 (2004).
[38] J. P. Perdew, K. Burke and M. Ernzerhof, Phys. Rev. Lett. **77**, 3865 (1996).
[39] P. E. Blöchl, Phys. Rev. B **50**, 17953 (1994).
[40] G. Kresse and J. Furthmüller, Phys. Rev. B **54**, 11169 (1996).
[41] G. Kresse and D. Joubert, Phys. Rev. B **59**, 1758 (1999).
[42] M.V. Nikolic, K. Satoh, T. Ivetic, K.M. Paraskevopoulos, T.T. Zorba, V. Blagojevic, L. Mancic, P.M. Nikolic, Thin Solid Films **516**, 6293 (2008)
[43] Y. Inaguma, M. Yoshida and T. Katsumata, J. Am. Chem. Soc. **130**, 6704 (2008).
[44] R. Dovesi, V. R. Saunders, C. Roetti, R. Orlando, C. M. Zicovich-Wilson, F. Pascale, B. Civalleri, K. Doll, N. M. Harrison, I. J. Bush, P. D'Arco, and M. Llunell, CRYSTAL09 User's Manual, University of Torino, Torino, 2009.
[45] W. J. Stevens, M. Krauss, H. Basch, and P. G. Jasien, Can. J. Chem. **70** 612 (1992).
[46] W. H. Press, B. P. Flannery, S. A. Teukolsky and W. T. Vettering, *Numerical Recipies*, chapter 10.7., Cambridge (1986).
[47] J. D. Gale, J. Chem. Soc., Faraday Trans. **93**, 629 (1997).
[48] D. Muñoz, A. Chroneos, M. J. D. Rushton and P. D. Bristowe, Thin Solid Films **555**, 117 (2014).
[49] W. Smith and I. T. Todorov, Mol. Simulat. **32** 935 (2006).
[50] R. H. Schröder, N. Schmitz-Pranghe and R. Kohlhaas, Z. Metallkd., **63**, 12, (1972).